Radiation Measurements 62 (2014) 52–59

Contents lists available at ScienceDirect

Radiation Measurements

journal homepage: www.elsevier.com/locate/radmeas

A method to enhance coincidence time resolution with applications for medical imaging systems (TOF/PET)

E.E. Ermis [a], C. Celiktas [a,*], E. Pilicer [b]

[a] Ege University, Faculty of Science, Physics Department, 35100 Bornova, Izmir, Turkey
[b] Uludag University, Faculty of Arts and Science, Physics Department, Gorukle, Bursa, Turkey

HIGHLIGHTS

- Two coincident inorganic scintillation detectors were used.
- Two coincident organic scintillation detectors were used.
- Timing method was utilized.
- Coincidence time resolution value for TOF/PET was enhanced.

ARTICLE INFO

Article history:
Received 13 February 2013
Received in revised form
26 December 2013
Accepted 21 January 2014

Keywords:
NaI(Tl) inorganic scintillation detector
BC418 type plastic scintillation detector
FLUKA Monte Carlo simulation program
TOF/PET

ABSTRACT

A coincidence timing spectrometer was assembled using NaI(Tl) inorganic and BC418 type organic (plastic) scintillation detectors. The constant fraction timing method was used. Coincidence time resolution values of the detectors, which have great importance in TOF/PET measurements, were obtained separately. The resolutions were enhanced using a different method in a start-stop coincidence spectrometer: the signals from the start detectors were delayed. The results from the FLUKA Monte Carlo simulation code agreed well with the experimental results.

© 2014 Elsevier Ltd. All rights reserved.

1. Introduction

It is often important to determine the time relationship of pulses in radiation measurements (Tsoulfanidis, 1995). For this purpose, the electronic determination of coincidence is used, e.g., coincidence in time between two events (Leo, 1994). Such coincidence measurements are also used in medical imaging systems. Imaging is becoming increasingly important in modern medicine, both as a means of diagnosis and as additional support for planning and controlling clinical procedures. Coincidence measurements have contributed to improvements in the quality of medical images. Enhanced contrast and resolution, reduced noise, distortion and artifacts have become key objectives in areas such as the physics of detectors and image reconstruction mathematics (De Lima, 2011). Medical imaging represents an increasingly important component of modern medical practice because early and accurate diagnoses can substantially influence patient treatment strategies (Iniewski, 2009). Medical imaging systems involve techniques ranging from simple planar and whole-body studies to positron emission tomography (PET) and single-photon emission computed spectroscopy (SPECT) (Iniewski, 2009; Yamada and Uchida, 2011). PET uses time of flight (TOF) information with fast scintillation detectors for human whole-body scans (Yamada and Uchida, 2011). In TOF measurement, the emitted photons are detected by two detectors (start and stop detectors). The detector signals are amplified and forwarded to a timing circuit. Currently, almost all commercially available scanners in PET systems employ scintillation crystals with photomultipliers (PMTs) to measure the radiation. In early PET systems, a single scintillator crystal was coupled to a single PMT. Sodium iodide NaI(Tl) is certainly the most popular detector crystal for the (non-PET) Anger camera. Modern PET systems use lutetium oxyorthosilicate (LSO), gadolinium oxyorthosilicate (GSO) or bismuth germanate (BGO); however, sodium iodide (NaI), cesium fluoride (CsF), and barium fluoride (BaF_2) have been tested for PET applications (Iniewski, 2009) as well.

The properties of imaging systems are usually expressed in physical terms. One of the concepts used to describe imaging

* Corresponding author.
E-mail addresses: cuneyt.celiktas@ege.edu.tr, cceliktas@yahoo.com (C. Celiktas).

1350-4487/$ – see front matter © 2014 Elsevier Ltd. All rights reserved.
http://dx.doi.org/10.1016/j.radmeas.2014.01.013

systems, in these terms, is spatial resolution. The spatial resolution of an imaging system is an important parameter: it corresponds to the minimum distance between two points in an object that allows the points to be observed as two distinct points in the image. This distance is parameterized by full width at half maximum (FWHM), the width of a peak at half its full height (De Lima, 2011). The time resolution of a timing system is defined as FWHM in the time spectrum (Fig. 1). Low time resolution value (a sharp peak in the time spectrum) indicates that the system has better time-detection sensitivity. Moreover, the FWHM value of a time distribution is also used as a measure of the overall timing uncertainty in the measurement system (Knoll, 2000). Spatial resolution (localization uncertainty of the coincidence system, Δx) can be defined as $\Delta x = c\Delta t/2$ in coincidence measurements (Ahmed et al., 2012; Choong, 2009; Snyder et al., 1981; Moses, 2003; Shibuya et al., 2010; Conti, 2009; Casey, 2008; Budinger, 1983; Conti et al., 2005; Karp et al., 2008), where c is the speed of the light (used because photons disperse at this speed) and Δt is time resolution of the system (error in time measurement). Another parameter of the coincidence measurement is the multiplicative reduction factor (f). This factor is calculated from $f = D/\Delta x$, where D is the size of the emission source or radial dimension of the object to be imaged (Choong, 2009; Moses, 2003, 2007; Conti, 2006). The square root of f ($\sqrt{f}$) is defined as the spatial resolution improvement (I), also called TOF gain, of a spectrometer (Choong, 2009; Conti, 2009, 2006; Budinger, 1983; Conti et al., 2005; Harrison et al., 2004). Higher I values mean better detection performance.

Peaking and shaping time are important parameters in a timing measurement. The peaking time is the time required for a pulse to reach its maximum amplitude (Knoll, 2000). The corresponding time to 61% of a timing peak value is defined as the shaping time. The peaking time is approximately 3–5 times greater than the shaping time (Fig. 1) (Bönisch, 2011).

The response times of the plastic scintillators are very short. Because of this property, scintillators are commonly used in time measurement and medical imaging experiments; for example, a PET camera is composed of an array of scintillation detectors surrounding an imaging volume (Iniewski, 2009; Yamada and Uchida, 2011; Takeshita et al., 2012; Miehe et al., 1966; Kelly et al., 1973). One of the scintillator types that has fast response times is an organic scintillator, such as the BC418 type plastic scintillator. The best time resolution can be obtained by using these scintillators because their decay times are very fast (1.4 ns) (Saint Gobain, 2013). The other type of scintillator is an inorganic scintillator such as NaI(Tl), where thallium (Tl) is an impurity activator. It has decay time of 250 ns at room temperature and is certainly the most popular detector for the medical imaging systems (De Lima, 2011; Iniewski, 2009).

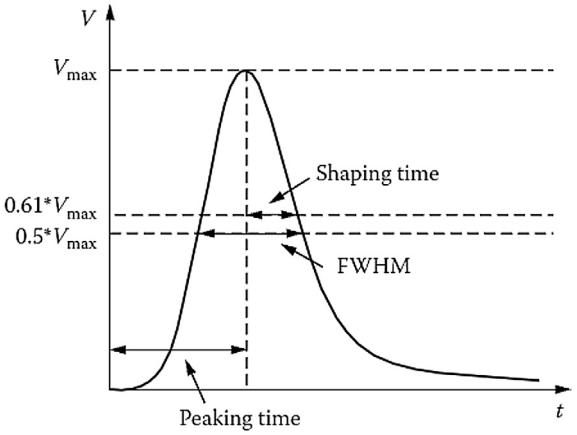


Fig. 1. Time spectrum, definitions of shaping and peaking times.

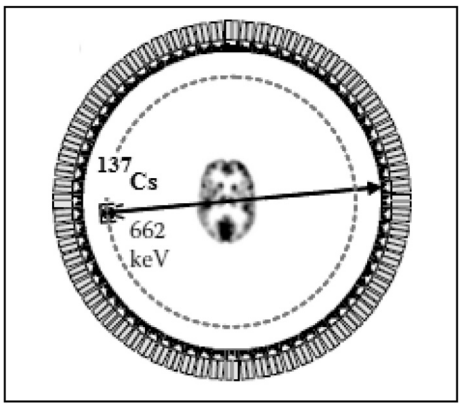


Fig. 2. The use of a ^{137}Cs radioactive source in medical imaging system.

The major reason for the design and development of the FLUKA Monte Carlo program is that the implementation and improvement of modern physical models are important. The interaction and propagation of any radiation in matter can be simulated using FLUKA (Ferrari et al., 2005; Battistoni et al., 2007).

Coincidence measurements and low background digital coincidence measurements using high-purity Ge (HPGe) detectors and a digitizer were conducted by Cizek et al. (Cizek et al., 2010, 2012). Ichihara et al. (2003) studied pulse shape discrimination method using NaI(Tl) detectors. The temperature dependence of the decay time constant of the NaI(Tl) detectors was examined using the pulse shape discrimination method of Schneid et al. (1977). Kelly et al. (1973) compared the scintillation lifetimes of various plastic scintillators such as Pilot U, M and B, Naton 136 and NE 111 using coincidence measurement. Miehe et al. (1966) studied resolving time values using plastic scintillation detectors. Shibuya et al. (2010) constructed a coincidence spectrometer of CsBr scintillators to investigate its timing performance. Borio di Tigliole et al. (2001) examined low-energy neutron interactions through experimental and theoretical methods. Korkut et al. (2011) determined the linear attenuation coefficient of a radiation shielding material using the FLUKA Monte Carlo program.

Medical imaging systems commonly consist of scintillator materials (Holstensson et al., 2008; Chaney et al., 1992; Xi et al., 2011; Chiang et al., 1983) because of their faster decay times. In a medical imaging system, the time resolution is an important parameter because image quality depends on it. Therefore, time resolution values should be determined very precisely. In the present study, a different experimental method is proposed to enhance the time resolution of a coincidence system. In the first part of the study, coincidence measurements were separately carried out using spectrometers consisting of NaI(Tl) and BC418 type plastic scintillation detectors by changing the distances between the source and the start detectors. The coincidence time resolution (or resolving time) and delay time for each distance were determined using the constant fraction timing method. In the second part of the study, time resolution was calculated by applying additional delay to the input of the timing signal to enhance the time and spatial resolutions of the spectrometers. The experimental results were compared with the results obtained using the FLUKA Monte Carlo program.

2. Materials and methods

A ^{137}Cs radioactive standard calibration source is a gamma emitter with a half-life of 30.07 years that produces single gamma photons with an energy of 662 keV (Fig. 2). This radionuclide is one

of the most commonly used sources in medical imaging (De Lima, 2011). In this work, the source's activity was 5 μCi.

Two Bicron NaI(Tl) and two BC418 plastic scintillation detectors were used in the experiments to obtain start-stop coincidence measurements. The detectors were constructed from the scintillators produced by Rexon Inc. (Beachwood, OH, USA). The NaI(Tl) and BC418 detectors had cylindrical and truncated cone shapes, respectively. Their dimensions are indicated in Fig. 3. The detectors were first placed 2 cm apart. The radioactive source was centered between them. This distance was chosen as reference

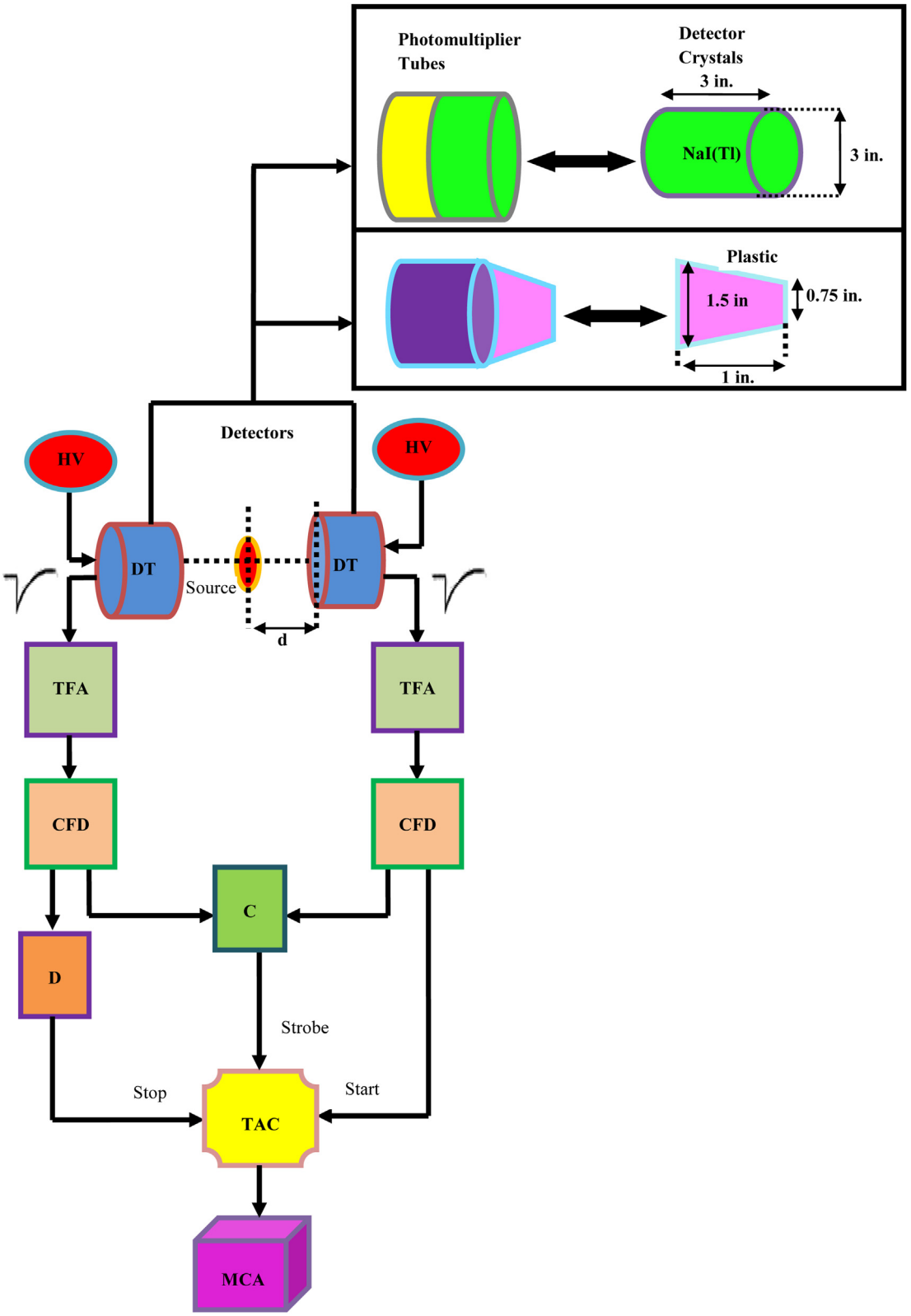


Fig. 3. Block diagram of the spectrometer.

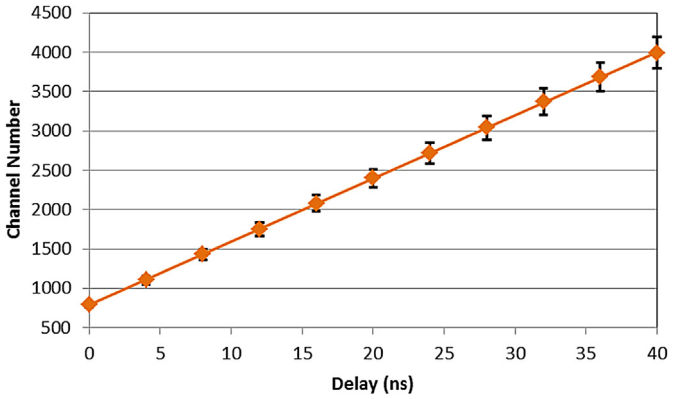


Fig. 4. Time calibration graph.

point. The start detector was moved $d = 2, 4, 6, 8$ cm from the source while the stop detector was fixed. The data acquisition time for the plastic detectors was chosen as 300 s. For NaI(Tl), 600 s was chosen because they recorded fewer counts than the plastic detectors. The measurements were taken in a dark room at constant temperature (22 °C) because ambient light and higher temperature caused detector noise (Leo, 1994).

Constant fraction timing is a method of timing measurement. The advantage of this method is a walk-free timing signal. It is important to exploit optimum triggering to obtain the best time resolution values (Leo, 1994). Further information about the method can be found in various references (Tsoulfanidis, 1995; Leo, 1994; Knoll, 2000; Nicholson, 1974).

The time spectra of ^{137}Cs were acquired using NaI(Tl) and plastic detector spectrometers. A block diagram of the spectrometers is illustrated in Fig. 3. The anode outputs (which give fast negative signals) of the photomultiplier tubes (PMT, Ortec 266) mounted on both detectors were connected to timing filter amplifiers (TFA, Ortec 454). The TFAs amplified the signals and reduced high-frequency noise by means of a selectable integration time (Bedwell and Paulus, 1976). The TFA outputs were sent to constant fraction discriminators (CFD, Ortec 463). A CFD module triggers on a constant fraction of the detector signal, independent of the signal amplitude (Vacik et al., 1998). One of the negative outputs of the CFDs was sent to the start input of a time to amplitude converter (TAC, Ortec 566). The negative output of the other CFD was connected to the stop input of the TAC through a delay unit (D, Ortec 425A) to ensure a time differences between its start-stop inputs. A TAC converts the time difference between two input signals to a voltage pulse whose height is proportional to the time between the signals. Consequently, a pulse whose height corresponds to a significant time value is generated (Tsoulfanidis, 1995). The coincident time spectrum of the two detectors was stored directly in a multichannel analyzer (MCA, Ortec Trump 8K). Positive outputs of both CFDs were sent to a coincidence module (C, Ortec 418A) to trigger the TAC through its strobe input. The logic output of the TAC was finally forwarded to the MCA in an attempt to achieve the time spectra. All connections between the modules used RG-58 C/U coaxial cables because fast negative timing signals were used.

The multichannel analyzer was first calibrated to determine the time value per channel. This time calibration graph can be observed in Fig. 4. The time per channel was determined by calculating the inverse of the slope of the time calibration graph, and it was found as 12.33 ± 0.12 ps/ch. The calibration was checked by dividing the range of TAC (100 ns) to the conversion gain of the MCA (8192 ch.), yielding 12.21 ps/ch. The two calibrations were nearly equal.

The same spectrometer was used with both types of detectors, as mentioned above. The detectors' positions were also simulated in FLUKA to check the validity of the experimental study using a theoretical method, as shown in Fig. 5.

The TFA output signal shapes from the NaI(Tl) and the plastic scintillation detectors are shown in Fig. 6. The peaking times for the NaI(Tl) and plastic scintillation detectors were determined to be 360 and 30 ns, respectively, via an oscilloscope with a sampling rate of 1 GS/s. The shaping times for the detectors were 120 and 6 ns, respectively.

The shape of the logic output of the TAC is shown in Fig. 7.

In the study, the start and stop detectors were first each placed 1 cm from the source. This distance was called the reference point ($d = 0$ cm). With the stop detector fixed, the start detector was moved to distances of $d = 2, 4, 6$ and 8 cm from the source. Time spectra were collected for each distance (d). It was observed that the channel numbers corresponding to the top positions of the timing peaks gradually moved to higher channel numbers as the start detector moved farther from the reference point. This movement showed that a time delay occurred with respect to the reference point when the start detector was farther from the reference point. This change of peak position (i.e., time delay) in the time spectrum was determined by subtracting the channel number of the peak positions of each distance from the channel number corresponding to the reference point. Thus, the change in channel numbers or delay time was determined experimentally for each distance.

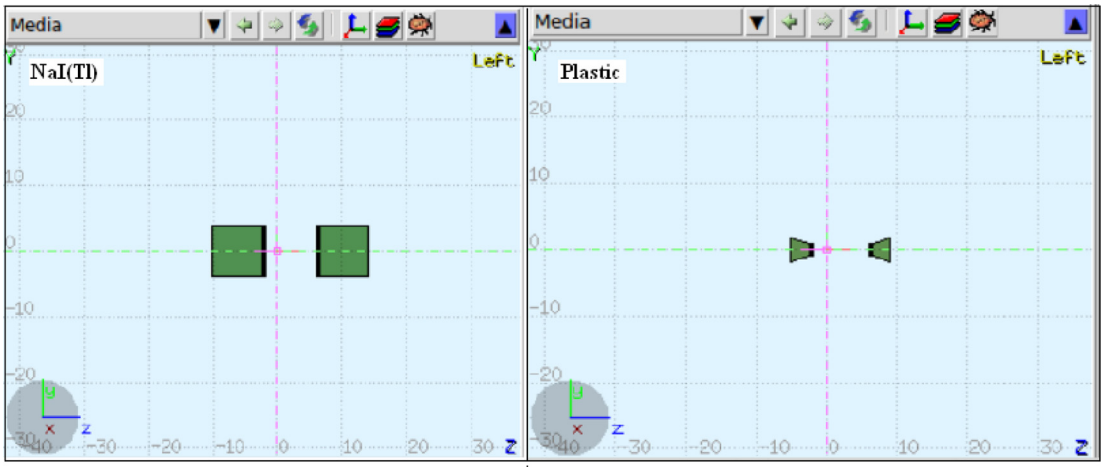


Fig. 5. Detectors' positions simulated in FLUKA program.

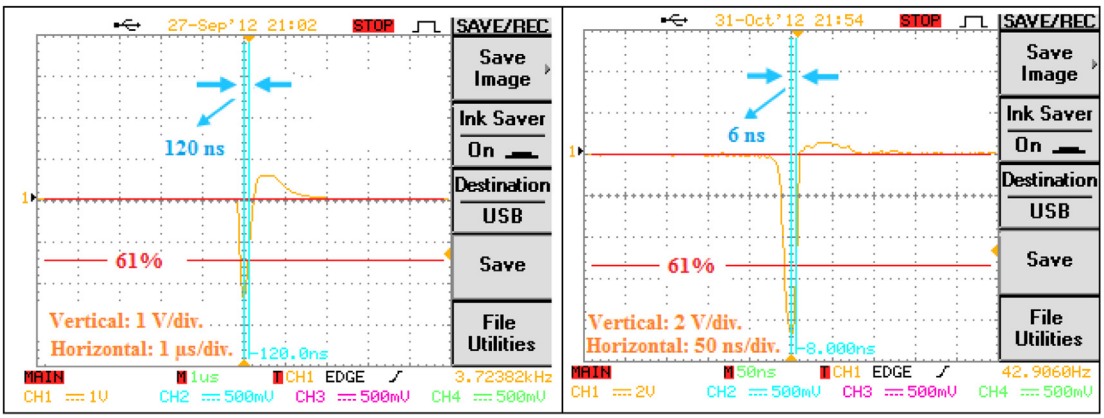


Fig. 6. Shaping times of (a) the NaI(Tl) and (b) the plastic scintillation detectors from the TFA.

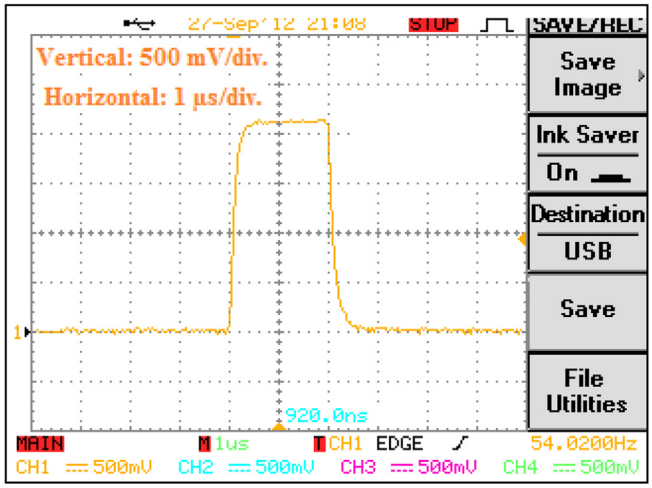


Fig. 7. TAC output signal shape.

A delay of 5 ns corresponds to 1 m-cable length for RG-58 C/U coaxial cables (Leo, 1994). From this information, the cable lengths were determined corresponding to the experimental delay times for each distance. In the second part of the study, cables of the determined length for each distance were added to the respective start inputs of the TAC to improve the time resolution. The time spectra were again acquired for both spectrometers. The results are given in the next section.

Maximum counts vs. distance from the reference point of the start detectors for both type detectors were also calculated using the FLUKA Monte Carlo program. The experimental and theoretical results are compared in the following sections.

3. Results

In Fig. 8, variations in the peak positions (in terms of channel number) versus distance from the reference point of the start detectors are shown.

The time resolution values obtained with and without additional delay cables at the start input of the TAC are shown in Figs. 9 and 10, respectively.

Experimental delay times were recorded from the MCA using the determined cable lengths. Additionally, these delay times were calculated using the information in (Leo, 1994). These experimental and theoretical delay time values are compared for both types of detectors in Figs. 11 and 12.

In the present study, the FLUKA program computed the maximum counts of the peak positions as a function of the distance from the reference point of the start detectors. These results are compared with the experiment in Figs. 13 and 14, respectively.

Using the equation given in the Introduction section, the spatial resolutions for the coincidence systems of plastic detectors with and without additional delay cable were found to be 22.59 and

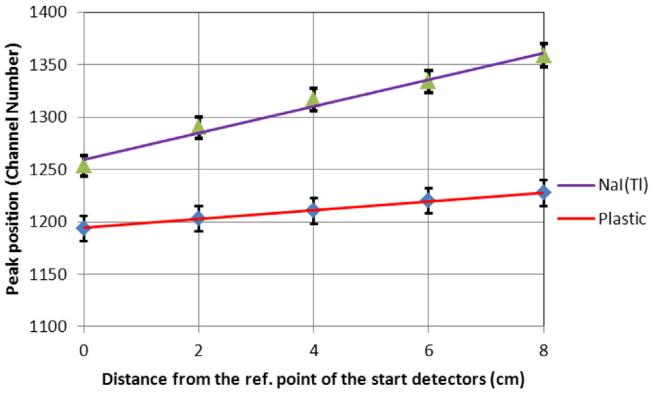


Fig. 8. Graph of distance from the ref. point of the start detectors vs. peak position for both detector types.

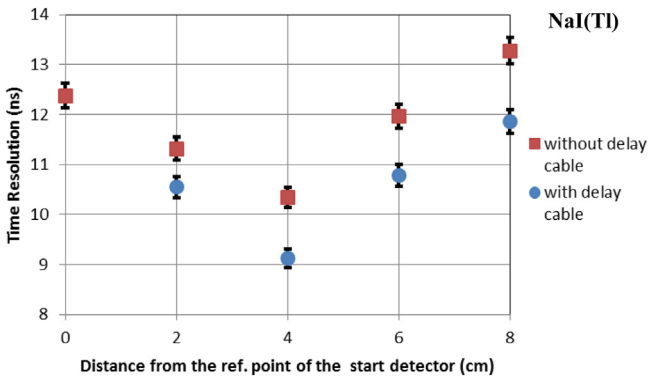


Fig. 9. Comparison of time resolution values without and with additional delay cables for the NaI(Tl) scintillation detectors.

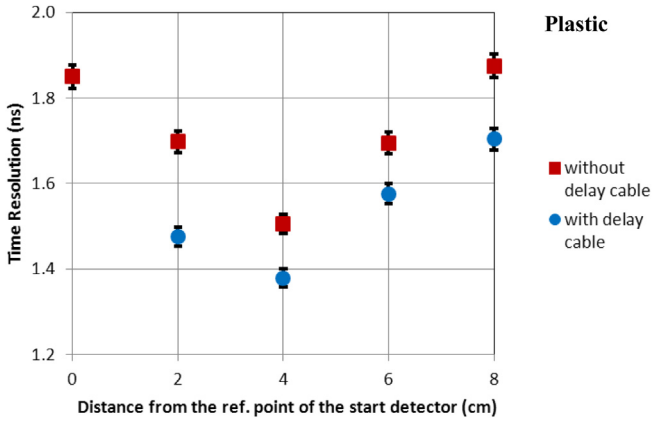


Fig. 10. Comparison of time resolution values without and with additional delay cables for the plastic scintillation detectors.

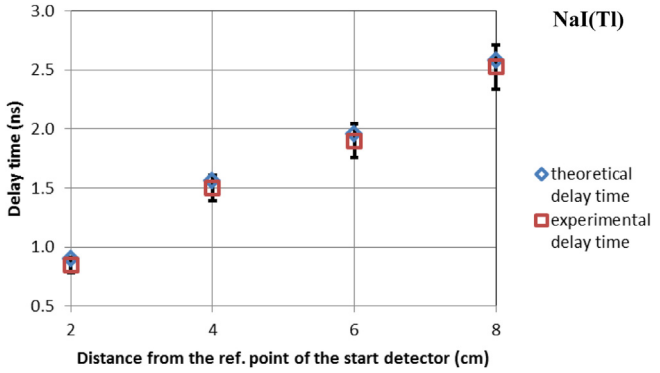


Fig. 11. Comparison of theoretical and experimental delay times for the NaI(Tl) scintillation detectors.

20.69 cm, respectively. Thus, the spatial resolution improvement for the spectrometer was approximately 8.4% over the whole-body imaging.

The f values calculated for the human whole-body ($D = 35$ cm) and brain ($D = 20$ cm) are indicated in Table 1. The positive effect of the additional delay can clearly be observed in the table.

Resolution improvement (I) values for the whole-body are also shown in Table 2.

It can be observed from this table that the additional delay to the start signal contributed to the time resolution improvement. In addition, time resolution values that were calculated for the

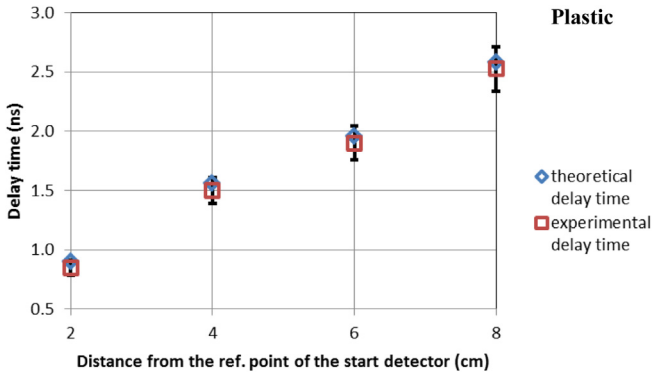


Fig. 12. Comparison of theoretical and experimental delay times for the plastic scintillation detectors.

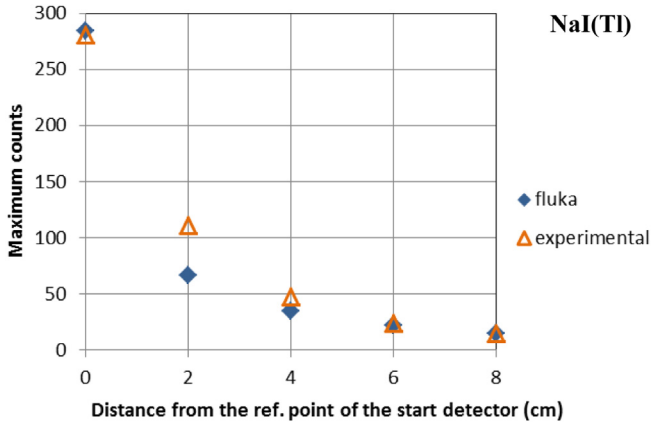


Fig. 13. Comparison of experimental and FLUKA maximum counts for the NaI(Tl) scintillation detectors.

coincidence systems with and without additional delay cables at various distances from the reference point of the start detector are tabulated in Table 3.

The delay times of the signals from the start detectors were calculated by subtracting the peak positions of the time spectrum corresponding to each distance from the peak positions of the reference points for both type detectors, so no time resolution values were normally written for the reference point in the first right cells in this table.

4. Conclusions and discussion

Time resolution is a crucial parameter for coincidence measurements in medical imaging systems such as TOF/PET because it affects the measurements' quality (Ahmed et al., 2012; Moses, 2003, 2007; Conti, 2009, 2006; Budinger, 1983; Conti et al., 2005). Therefore, this work investigated the optimum time resolution values for a start-stop coincidence timing spectrometer using the constant fraction timing method. Time spectra were obtained using NaI(Tl) and BC418 type plastic scintillation detector spectrometers. A different coincidence method and a spectrometer composed of organic plastic detectors (BC418) were suggested. The results obtained using the plastic detectors were better than the results obtained using the NaI(Tl) scintillation detectors, especially in whole-body imaging. Therefore, it was determined that the BC418 type plastic detectors were quite suitable for TOF/PET systems.

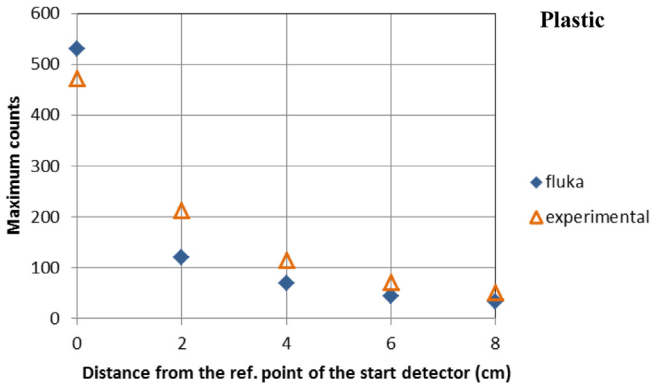


Fig. 14. Comparison of experimental and FLUKA maximum counts for the plastic detectors.

Table 1
f Values of the coincidence systems with and without additional delay cables.

Detectors	*f* Value for whole-body		*f* Value for human brain	
	Without delay cable	With delay cable	Without delay cable	With delay cable
NaI(Tl)	0.21	0.26	0.12	0.15
Plastic	1.55	1.69	0.89	0.97

Table 2
Resolution improvement values of the coincidence systems with and without additional delay cables.

Detectors	Resolution improvement (I) (for whole-body, $D = 35$ cm)	
	Without additional delay cable	With additional delay cable
NaI(Tl)	1.24	1.30
Plastic	0.45	0.51

The time and spatial resolution of coincidence systems, e.g., TOF and PET, have been investigated in various studies (Ahmed et al., 2012; Choong, 2009; Snyder et al., 1981; Moses, 2003; Shibuya et al., 2010). An improved time resolution in these systems would result in better medical imaging. In the present work, to enhance the time resolution of a coincidence spectrometer, the fast signal from the start detector at different distances from the reference point was delayed before the timing process. This delay improved the spectrometers' time resolution, as shown in Table 3. Thus, a different method was used in a timing coincidence spectrometer with the additional delay cables.

Time resolution of the plastic detectors was normally better than that of the NaI(Tl) scintillation detectors (Table 3) because of their lower decay times. In addition, resolution with delay cables improved over that without delay cables (Table 2). It can be concluded that the proposed timing method was highly successful in enhancing the coincidence time resolution. This method should thus lead to improved medical image quality.

The distances from the reference point of both types of start detectors were increased to 2, 4, 6 and 8 cm. The best time resolution values with and without additional delay cables were surprisingly obtained with 4 cm between the source and the start detectors (Figs. 9 and 10, Table 3).

A comparison of theoretical and experimental delay times for both detectors was made (Figs. 11 and 12). The delay times were found to be close to each other. This finding demonstrates that the experimental results with the additional cable length are reliable. In addition, the maximum counts for each distance from the reference point of the start detectors from the FLUKA program and the experimental study for both detector types were consistent (Figs. 13 and 14).

Table 3
Experimental time resolution results of the coincidence systems with and without additional delay cables with respect to the distance from the reference point of the start detectors.

Distance from the ref. point of the start detectors (d) (cm)	Time resolution (without additional delay cable) (ns)		Time resolution (with additional delay cable) (ns)	
	NaI(Tl)	Plastic	NaI(Tl)	Plastic
0.0	12.378 ± 0.284	1.850 ± 0.188	–	–
2.0	11.315 ± 0.297	1.698 ± 0.120	10.546 ± 0.308	1.475 ± 0.124
4.0	10.339 ± 0.311	1.506 ± 0.167	9.120 ± 0.331	1.379 ± 0.085
6.0	11.957 ± 0.289	1.695 ± 0.198	10.784 ± 0.305	1.576 ± 0.059
8.0	13.272 ± 0.274	1.875 ± 0.236	11.862 ± 0.290	1.704 ± 0.078

When the spatial resolution and *f* values for both detector types for ^{137}Cs were compared with Ref. (Moses, 2003, 2007; Karp et al., 2008), whole-body imaging could be achieved using the spectrometers used in this study. Benefitting from the experience and results obtained in the present study, further studies will continue with a positron source to consolidate the validity of the method proposed here.

This work demonstrated that the time resolution of a start-stop coincidence system was enhanced by using a different method. Based on the results of the spatial resolution calculation, it can be deduced that whole-body and brain imaging can be achieved using a TOF/PET spectrometer that consists of a BC418 type plastic scintillation detector.

Acknowledgment

This work was supported by TUBITAK, the Scientific and Technological Research Council of TURKEY under Project No. 197T087 and by EBILTEM, Center of Science and Technology, Ege University under Project No. 99 BIL 001.

References

Ahmed, M., Camanzi, B., Matheson, J., 2012. Characterisation of silicon photomultipliers for time-of-flight. PET Nucl. Instrum. Meth. A 695, 252–256.
Battistoni, G., Cerutti, F., Fasso, A., Ferrari, A., Muraro, S., Ranft, J., Roesler, S., Sala, P.R., 2007. Proceedings of the Hadronic shower simulation. Workshop 2006 Fermilab. In: Albrow, M., Raja, R. (Eds.), AIP Conference Proceeding, vol. 896, pp. 31–49.
Bedwell, M.O., Paulus, T.J., 1976. A new constant fraction timing system with improved time derivation characteristics. IEEE Trans. Nucl. Sci. 23, 234–243.
Bönisch, S.P., 2011. Electronics for Radiation Detection. CRC Press, USA.
Borio di Tigliole, A., Cesana, A., Dolfini, R., Ferrari, A., Raselli, G.L., Sala, P., Terrani, M., 2001. FLUKA simulations for low-energy neutron interactions and experimental validation. Nucl. Instrum. Meth. A 469, 347–353.
Budinger, T., 1983. Time-of-flight positron emission tomography: status relative to conventional PET. J. Nucl. Med. 24, 73–78.
Casey, M.E. Improving PET with HD PET + Time of flight http://www.medical.siemens.com/siemens/de_DE/gg_nm_FBAs/files/brochures/2008/ultraHD-PET_White_Paper.pdf (accessed 12.02.13).
Chaney, R.C., Fenyves, E.J., Hammack, H., Nelson, G., Anderson, J.A., Antich, P.P., Atac, M., 1992. Testing of the spatial resolution and efficiency. IEEE Trans. Nucl. Sci. 39, 1472–1474.
Chiang, B.S., Gautam, S.R., Hopkins, F.F., Morgan, I.L., 1983. Spatial resolution in industrial tomography. IEEE Trans. Nucl. Sci. 30, 1671–1676.
Choong, W.S., 2009. The timing resolution of scintillation-detector systems: Monte Carlo analysis. Phys. Med. Biol. 54, 6495–6513.
Cizek, J., Vicek, M., Prochazka, I., 2010. Digital spectrometer for coincidence measurement of doppler broading of positron annihilation radiation. Nucl. Instrum. Meth. A 623, 982–994.
Cizek, J., Vicek, M., Lukac, F., Melikhova, O., Prochazka, I., Anwand, W., Butterling, M., Wagner, A., Brauer, G., 2012. Low background digital coincidence spectrometer – a tool for investigation of positron annihilation in flight. Diffus. Defect Data Pt. A 331, 53–73.
Conti, M., 2006. Effect of randoms on signal-to-noise ratio in TOF PET. IEEE Trans. Nucl. Sci. 53, 1188–1193.
Conti, M., 2009. State of the art and challenges of time-of-flight PET. Phys. Med. Eur. J. Med. Phys. 25, 1–11.
Conti, M., Bendriem, B., Casey, M., Chen, M., Kehren, F., Michel, C., Panin, V., 2005. First experimental results of time-of-flight reconstruction on an LSO PET scanner. Phys. Med. Biol. 50, 4507–4526.
De Lima, J.J.P., 2011. Nuclear Medicine Physics. Taylor & Francis, USA.
Ferrari, A., Sala, P.R., Fasso, A., Ranft, J., 2005. Fluka: A Multi-particle Transport Code CERN.
Harrison, R.L., Alessio, A.M., Kinahan, P.E., Lewellen, T.K., 2004. Signal to noise ratio in simulations time-of-flight positron emission tomography. In: IEEE Nucl. Sci. Symposium Conference Record, pp. 4080–4083.
Holstensson, M., Partridge, M., Buckly, S.E., Flux, G.D., 2008. The effect of energy on scintillation camera intrinsic spatial resolution. IEEE Nucl. Sci. Symposium Conference Record, 4811–4813.
Ichihara, K., Fushimi, K., Koori, N., Nakayama, S., Takahisa, K., Umehara, S., Yoshida, S., 2003. Highly sensitive measurement of α-rays in NaI(Tl) scintillator by pulse shape discrimination with charge-sensitive analog-to-digital converter. Nucl. Instrum. Meth. A 515, 651–656.
Iniewski, K., 2009. Medical Imaging Principles, Detectors and Electronics. John & Sons Inc., New York.

Karp, J.S., Surti, S., Daube-Witherspoon, M.E., Muehllehner, G., 2008. Benefit of time-of-flight in PET: experimental and clinical results. J. Nucl. Med. 49, 462–470.
Kelly, T.M., Merrigan, J.A., Lambrecht, R.M., 1973. Comparison of plastic scintillators with nanosecond lifetimes. Nucl. Instrum. Meth. A 109, 233–235.
Knoll, G.F., 2000. Radiation Detection and Measurements. John& Sons Inc., New York.
Korkut, T., Korkut, H., Karabulut, A., Budak, G., 2011. A new radiation shielding material: amethyst ore. Ann. Nucl. Energy 38, 56–59.
Leo, R.W., 1994. Techniques for Nuclear and Particle Physics Experiments. Springer-Verlag, Germany.
Miehe, J.A., Ostertag, E., Coche, A., 1966. Measurement of resolving times with the fast RCA C-70045 photomultipliers. IEEE Trans. Nucl. Sci. 13, 127–131.
Moses, W.W., 2003. Time of flight in PET revisited. IEEE Trans. Nucl. Sci. 50, 1325–1330.
Moses, W.W., 2007. Recent advances and future advances in time-of-flight PET. Nucl. Instrum. Meth. A 580, 919–924.
Nicholson, P.W., 1974. Nuclear Electronics. John & Sons Inc., New York.
Saint-Gobain Plastic Scintillator. http://www.detectors.saint-gobain.com/Plastic-Scintillator.aspx (accessed 12.02.13).
Schneid, E.J., Kamykowski, E.A., Swanson, F.R., 1977. Influence of the temperature dependence of the NaI(Tl) decay time constant on NaI(Tl) detector application. IEEE Trans. Nucl. Sci. 24, 168–171.
Shibuya, K., Saito, H., Koshimizu, M., Asai, K., 2010. Outstanding timing resolution of pure CsBr scintillators for coincidence measurements of positron annihilation radiation. Appl. Phys. Express 3, 086401–086403.
Snyder, D.L., Thomas, L.J., Ter-Pogossian, M.M., 1981. A mathematical model for positron-emission tomography systems having time-of-flight measurements. IEEE Trans. Nucl. Sci. 28, 3575–3583.
Takeshita, T., Yamazaki, M., Yoji, H., 2012. Study of TOF-PET performance. Phys. Proc. 37, 1461–1465.
Tsoulfanidis, N., 1995. Measurements and Detection Radiation. Taylor & Francis, USA.
Vacik, J., Cervena, J., Hnatowicz, V., Havranek, H., Hoffmann, J., Posta, S., Fink, D., Klett, R., 1998. Pulse-shape discrimination in neutron depth profiling technique. Nucl. Instrum. Meth. B 142, 397–401.
Xi, D., Liu, J., Li, Y., Zhu, J., Niu, M., Xiao, P., Xie, Q., 2011. Investigation of continuous scintillatior/SiPM detector for local extremely high spatial resolution PET. IEEE Nucl. Sci. Symp. Conf. Rec., 4429–4432.
Yamada, R., Uchida, H., 2011. Electronics for Radiation Detection. CRC Press, USA.